JTTEE 3:69-74
©ASM International

A Taguchi Experimental Design Study of Twin-Wire Electric Arc Sprayed Aluminum Coatings

D.J. Varacalle, Jr., G.C. Wilson, R.W. Johnson, T.J. Steeper, G. Irons, W.R. Kratochvil, and W.L. Riggs

An experimental study was conducted on the twin-wire electric arc spraying of aluminum coatings. This aluminum wire system is being used to fabricate heater tubes that emulate nuclear fuel tubes for use in thermal-hydraulic experiments. Experiments were conducted using a Taguchi fractional factorial design parametric study. Operating parameters were varied around the typical process parameters in a systematic design of experiments to display the range of processing conditions and their effect on the resultant coating. The coatings were characterized by hardness tests, optical metallography, and image analysis. This article discusses coating hardness, roughness, deposition efficiency, and microstructure. The study attempts to correlate the features of the coatings with the changes in operating parameters. A numerical model of the process is presented, including gas, droplet, and coating dynamics.

1. Introduction

Thermal spraying is a generic term that encompasses several material spraying processes: plasma spraying, combustion (flame) spraying, nozzle aspirated spraying, and electric arc spraying.[1-3] The more common thermal spray coating functions include wear resistance, heat and oxidation resistance, corrosion resistance, electrical or thermal conductivity or resistivity, restoration of dimension, and clearance control.

In the electric arc spray process, two wires are brought together, and an electric arc is struck between them. Typical dc voltages are between 25 and 35 V, with current ranging up to 350 A or more. The arc developed between the two wires causes the tips of the wires to melt. An atomizing gas, generally air, is delivered to the wires in such a way as to strip off small droplets of molten metal. In this way, kinetic energy is delivered to the droplets. Gases other than air may be substituted. Either nitrogen or argon may be sprayed to reduce the formation of oxide on the molten droplets. As material is removed, additional material is supplied by a controlled means of delivering the wires. The spatial separation of the wires is determined by adjusting the voltage (i.e., the potential drop across the wires). For different materials, the optimal values of voltage, current, and air pressure can be determined, although typical values range from 25 to 35 V, 100 to 250 A, and 30 to 60 scfm of air (850 to 1699 l/min), respectively. In general, any material that is electrically conductive and can be made into a wire can be sprayed with a twin-wire electric arc device.

Key Words: aluminum coatings, optimization, processing parameters, Taguchi method, twin-wire electric arc

T.J. Steeper, Savannah River Laboratory, Aiken, South Carolina; **D.J. Varacalle, Jr., G.C. Wilson,** and **R.W. Johnson,** Idaho National Engineering Laboratory, EG&G Idaho, Inc., P.O. Box 1625, Idaho Falls, ID 83415; **G. Irons** and **W.R. Kratochvil,** Hobart-Tafa Corp., Concord, NH 03301; and **W.L. Riggs, II,** TubalCain Company, Loveland, OH 45140.

Thermal spray technology is used to fabricate heater tubes for thermal-hydraulic experiments.[4,5] These heaters are fabricated using a multilayered coating system consisting of a bond coat, ceramic insulator, metal conductor, second ceramic insulator, and an aluminum skin. A twin-wire electric arc system is used to fabricate the heater skin. The aluminum skin has to withstand a water/steam environment and prevent any leakage into the inner conductor, which could result in shorting of the heater. Thus, minimum porosity is required. Also, the heater requires the thermal properties of pure aluminum. The arc spray process was chosen for its ability to fabricate high-purity aluminum coatings, with high bond and interparticle strength. For this application, porosity and cracking of the aluminum are the most important microstructural features that must be minimized for the construction of durable heaters. This work attempts to further the scientific understanding of the physical mechanisms involved in the formation of twin-wire electric arc metal coatings by determining which processing parameters affect the structure and properties of the coatings.

2. Experimental Procedures

A statistical design of experiment approach was used to optimize the aluminum skin layer of the heater tubes. Figure 1 illustrates a typical fabricated heater tube. A Hobart-Tafa twin-wire electric arc spray system and commercially available thermal spray aluminum wire (Tafa 01T) were used for this study.

Three Taguchi[6] L4 experiments were conducted. Each experiment evaluated the effect of three processing variables on the quantitatively measured responses. System currents of 150, 250, and 300 A were used.

The statistical design of experiment evaluation of the thermal spray process is ideal because it displays the range of measured coating characteristics attainable, and it statistically delineates the impact of each factor on the measured coating characteristics across all combinations of other factors. This information is use-

ful in examining the physical principles involved in thermal spray coatings, establishing realistic coating specifications, and developing new equipment. The Taguchi analysis was accomplished with personal computer-based software[7] on the measured responses.

Experiments TA01 through TA15 represent the 15 experiments. In the three Taguchi schemes, each variable has two levels selected to band around the nominal settings (i.e., Experiment TA01 for Experiments TA02 through TA05, Experiment TA06 for Experiments TA07 through TA10, Experiment TA11 for experiments TA12 through TA15) to demonstrate the processing capabilities at a variety of stable thermal conditions. The experiments are detailed in Table 1. The parameters varied were primary air flow, spray distance, and gun traverse rate. Experiments TA01 through TA05 used a current of 150 A. Experiments TA06 through TA10 used 250 A. Experiments TA11 through TA15 used 300 A. The resulting responses evaluated were thickness (optical microscopy), superficial hardness (Rockwell 15T test), microhardness (Vickers test HV300), porosity and coating roughness (image analysis), and deposition efficiency.

Air was used for the atomizing gas in the twin-wire electric arc spray system. Wire feed was 19.8 kg/h (9 lb/h) for the 150 A experiments, 6.8 kg/h (15 lb/h) for the 250 A experiments, and 8.2 kg/h (18 lb/h) for the 300 A experiments. An x-y manipulator ensured the standoff distance and repeatability in the experiments. A y-step of 3.2 mm (0.125 in.) was used. Each cycle consisted of 12 traverses. Three cycles were used to fabricate coatings TA01 through TA05, and two cycles were used to fabricate coatings TA06 through TA15. A system voltage of 28 V was used for all experiments. The wire was thermal sprayed onto 6061 aluminum coupons (51 × 63 × 3 mm, or 2 × 2 × 0.125 in.) which were cooled by air jets on the back side. One side of each steel coupon was grit blasted with No. 30 alumina grit before spraying.

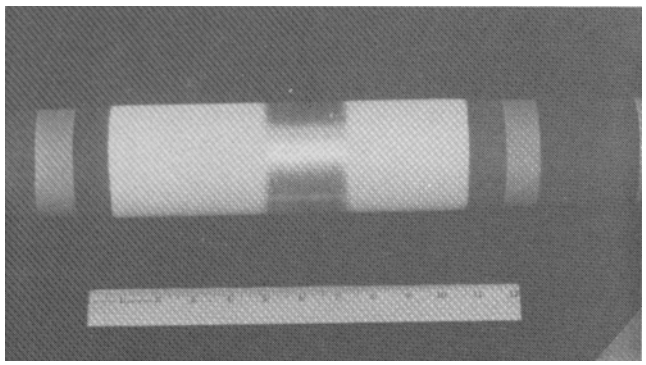

Fig. 1 Typical heater tube

3. Materials Characterization Results

Table 2 lists the coating characterization results for this study. The coating thicknesses, as revealed by optical metallographic observations at 300× magnification, are also listed in Table 2. This table lists average thicknesses from 12 measurements of the aluminum layers, which account for the influence of the various spraying parameters. Thickness per pass ranged from 3.2 to 10 mils (81 to 255 μm).

Porosity values for the coatings, as revealed by image analysis, are listed in Table 2. A Dapple image analyzer with a Nikon Epiphot metallograph was used for the metallurgical mounts. Image analysis procedures were first tested for sensitivity to parameter variation. The average porosity of the aluminum coatings ranged from 2.7 to 6.2%.

The coatings were measured for superficial Rockwell hardness and microhardness. Twelve measurements were taken and averaged. The superficial Rockwell hardness measurements, taken normal to the deposit using the 15T method, ranged from 23 to 60. Microhardness measurements (i.e., HV300), taken on a ground and polished cross section through the coating, ranged from 41.7 to 52.6.

Deposition efficiency, ranging from 46.3 to 57.8%, was determined by measuring the amount of sprayed metal deposited for an allotted time. Surface roughness, as determined by image analysis, ranged from 5.52 to 7.65 μm; higher values are rougher.

Table 1 Aluminum twin-wire electric arc Experiments TA01 through TA15

Experiment No.	Taguchi	Current(a), A	Console P/Q(b,c)	Traverse rate(d) in./s	Traverse rate(d) mm/s	Standoff mm	Standoff in.
TA01	(e)	150	45(310.5)/47.8	18.0	457.2	152.4	6.0
TA02	1-1-1	150	40(276)/43.8	15.0	381.0	127.0	5.0
TA03	1-2-2	150	40(276)/43.8	21.0	533.4	177.8	7.0
TA04	2-1-2	150	50(345)/50.5	15.0	381.0	177.8	7.0
TA05	2-2-1	150	50(345)/50.5	21.0	533.4	127.0	5.0
TA06	(e)	250	45(310.5)/47.8	18.0	457.2	152.4	6.0
TA07	1-1-1	250	40(276)/43.8	15.0	381.0	127.0	5.0
TA08	1-2-2	250	40(276)/43.8	21.0	533.4	177.8	7.0
TA09	2-1-2	250	50(345)/50.5	15.0	381.0	177.8	7.0
TA10	2-2-1	250	50(345)/50.5	21.0	533.4	127.0	5.0
TA11	(e)	300	45(310.5)/47.8	18.0	457.2	152.4	6.0
TA12	1-1-1	300	40(276)/43.8	15.0	381.0	127.0	5.0
TA13	1-2-2	300	40(276)/43.8	21.0	533.4	177.8	7.0
TA14	2-1-2	300	50(345)/50.5	15.0	381.0	177.8	7.0
TA15	2-2-1	300	50(345)/50.5	21.0	533.4	127.0	5.0

(a) Gun current in amperes. **(b)** Console pressure in psia and kPa (in parentheses). **(c)** Console flow in liters/min. **(d)** Gun traverse rate in in./s. **(e)** Equipment manufacturer's recommended process parameters.

Table 2 Coating characterization results for Experiments TA01 through TA15

Experiment No.	Thickness				Hardness, HRC 15T	Hardness, VH(a)	Porosity, %	Deposition efficiency, %	Roughness, μm
	μm	mils	μm/pass	mils/pass					
TA01	363	14.3	122	4.8	49	45.4	4.8	51.1	5.70
TA02	473	18.6	158	6.2	53	52.6	6.2	53.5	6.27
TA03	244	9.6	81	3.2	54	50.8	4.4	46.3	6.00
TA04	396	15.6	132	5.2	41	46.8	4.7	47.7	5.52
TA05	366	14.4	122	4.8	53	46.3	5.7	54.8	5.55
TA06	338	13.3	170	6.7	60	44.8	4.8	51.5	6.42
TA07	440	17.3	221	8.7	34	41.7	5.0	57.0	7.51
TA08	244	9.6	122	4.8	53	48.6	4.8	46.4	6.76
TA09	368	14.5	186	7.3	57	41.9	3.0	49.0	5.94
TA10	313	12.3	158	6.2	49	46.6	4.8	55.4	6.10
TA11	424	16.7	214	8.4	43	44.4	3.4	52.8	5.85
TA12	508	20.0	255	10.0	31	44.8	4.4	57.0	6.25
TA13	315	12.4	158	6.2	37	44.1	4.0	49.0	6.73
TA14	361	14.2	181	7.1	23	42.2	2.7	48.8	6.05
TA15	391	15.4	196	7.7	27	44.0	3.7	7.8	7.65

(a) Vickers microhardness values (300-g load).

Table 3 Results of the Taguchi analysis at 150 A

Desired attribute	Processing factor		
	Gun pressure, ρ%/psia	Traverse rate, ρ%/in./s	Spray distance, ρ%/in.
Low porosity	0.5/50	7.5/21	92.0/7
High thickness	1.9/50	61.9/15	36.2/5
Low roughness	90.7/50	3.6/21	5.7/7
High hardness (Rockwell)	36.8/40	36.8/21	26.4/5
High microhardness	93.8/40	4.7/15	1.5/5

Table 4 Results of the Taguchi analysis at 250 A

Desired attribute	Processing factor		
	Gun pressure, ρ%/psia	Traverse rate, ρ%/in./s	Spray distance, ρ%/in.
Low porosity	37.9/50	24.2/15	37.9/7
High thickness	0.0/40	76.4/15	23.6/5
Low roughness	80.9/50	5.7/21	13.5/7
High hardness (Rockwell)	29.8/50	10.0/21	60.2/7
High microhardness	2.3/40	94.3/21	3.4/7

The data from each image were mathematically treated according to ANSI Standard B46.1 in which roughness is calculated as the average departure y from the mean height in a given region. The average departure y was determined for 20 frames, and the 20 frames were averaged to yield the final measured roughness.

Image analysis revealed variations in the microstructures of the coatings for the experiments. The combination of 345 kPa (50 psia) console pressure, 381 mm/s (15 in./s) traverse rate, and 177.8 mm (7 in.) spray distance produced thick coatings with the lowest porosity and lowest roughness for each Taguchi experiment. Figure 2 illustrates microstructures for coatings TA04, TA09, and TA14. Comparison of the coatings indicates that porosity decreased as current increased (i.e., going from 150, to 250, to 300 A). Surface roughness for the three best coatings was not significantly different.

Table 5 Results of the Taguchi analysis at 300 A

Desired attribute	Processing factor		
	Gun pressure, ρ%/psia	Traverse rate, ρ%/in./s	Spray distance, ρ%/in.
Low porosity	69.5/50	3.9/15	26.6/7
High thickness	6.2/40	32.5/15	61.3/5
Low roughness	8.5/40	70.9/15	20.6/7
High hardness (Rockwell)	75.7/40	23.4/21	0.9/7
High microhardness	49.4/40	8.2/21	42.4/5

4. Discussion of Taguchi Fractional Factorial Experiment Design

The spray tests were conducted and evaluated once, and all data points were considered in the analysis of variance (ANOVA) calculations. The rho percent (ρ%) calculation indicates the influence of a factor or parameter on the measured response, with a larger number indicating more influence. The ANOVA calculations guide further experimentation by indicating which parameters are the most influential on coating attributes. This information is very useful in developing new coating specifications.

The optimum coating for this application (as shown in Table 3 in order of priority) would have low porosity, high thickness, low roughness, high hardness, and a high deposition efficiency. Tables 3, 4, and 5 illustrate the results of the Taguchi analysis.

The three Taguchi experiments indicated different trends for lowering porosity in the coatings. At 150 A, spray distance was the most significant contributor to lowering porosity at 92 ρ%, with the longer standoff (177.8 mm, or 7 in.) resulting in lower porosity. Other contributors were traverse rate at 7.5 ρ%, with the higher rate (533.4 mm, or 21 in./s) resulting in lower poros-

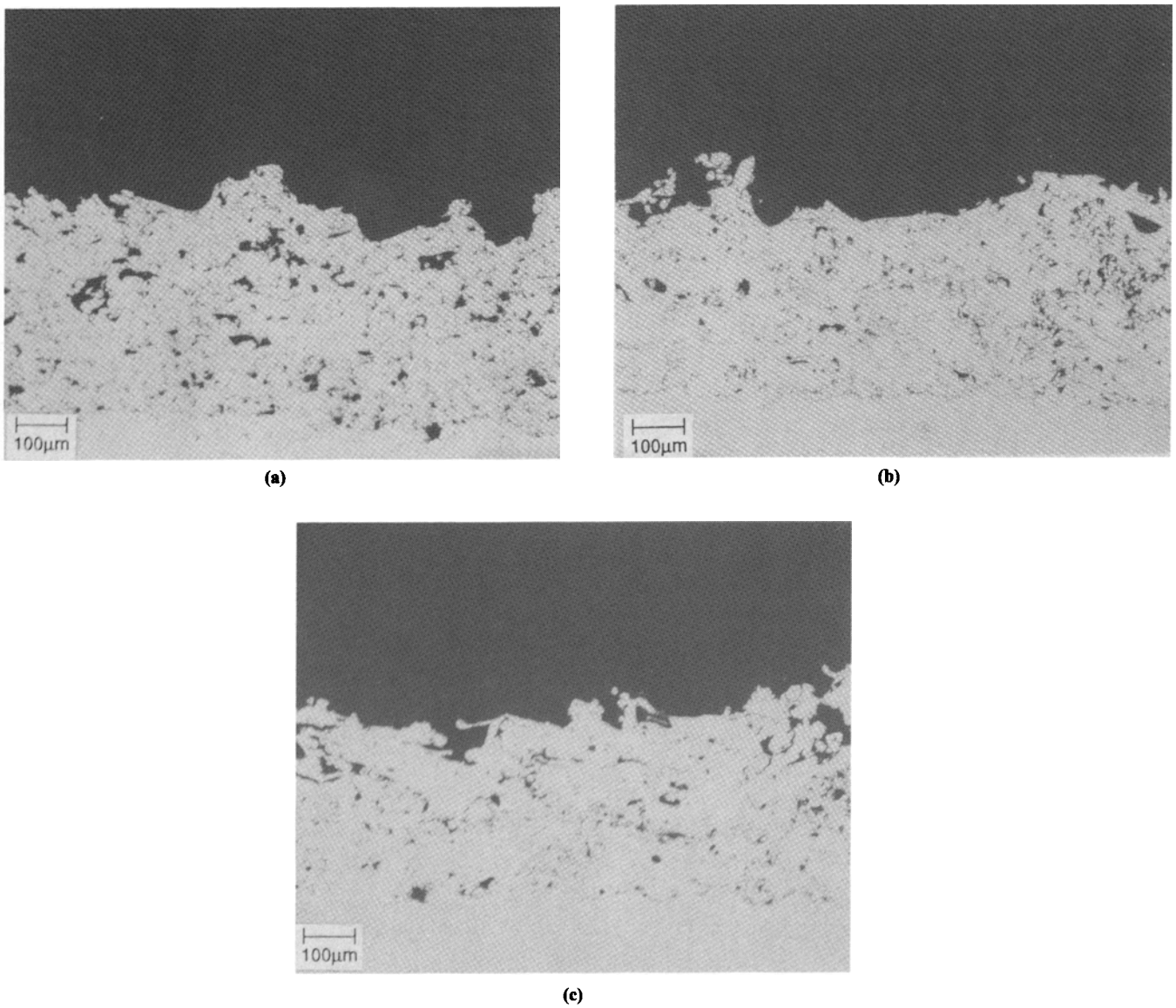

Fig. 2 Optical photomicrographs of as-sprayed coatings TA04, TA09, and TA14 at 200×

ity. At 250 A, gun pressure and spray distance were the most significant contributors to lowering porosity at 37.9 ρ% each, with the greater standoff (177.8 mm, or 7 in.) and higher gun pressure (345 kPa, or 50 psia) resulting in lower porosity. Traverse rate was 24.2 ρ%, with the lower rate (381 mm/s, or 15 in./s) resulting in lower porosity. At 300 A, only gun pressure was significant for lowering porosity at 69.5 ρ%; the higher gun pressure (345 kPa, or 50 psia) resulted in lower porosity. Spray distance contributed to a lesser extent at 26.6 ρ%, with the longer standoff (177.8 mm, or 7 in.) resulting in lower porosity.

Coating thickness buildup is dominated by wire feed rate, which is dictated by the system current. Higher current results in faster wire feed and thicker coatings. This trend appeared when the thicknesses deposited per pass were compared among cases where all variables were constant except for increasing current (e.g., Experiments TA01, TA06, TA11; TA02, TA07, TA12). The Taguchi evaluation at 150 A indicated that slower gun traverse rate was the most significant contributor to increasing thickness at 61.9 ρ%; the shorter spray distance (127mm, or Sin.) was next most significant at 36.2 ρ%. At 250 A, traverse rate was the most significant contributor to increasing thickness at 76.4 ρ%, with the slower traverse rate (381 mm/s, or 15 in./s) resulting in greater thickness. Spray distance at 23.6 ρ% was a less significant contributor, with the shorter standoff (127 mm, or 5 in.) resulting in greater thickness. At 300 A, spray distance was the most significant contributor to increasing thickness at 61.3 ρ%, with the shorter distance (127 mm, or 5 in.) resulting in greater thickness. Traverse rate at 32.5 ρ% was a less significant contributor, with the slower traverse (381 mm/s, or 15 in./s) resulting in greater thickness.

Surface roughness was reduced by using the higher level for gun pressure at 150 A (90.7 ρ%). The Taguchi evaluation at 250 A also indicated that primarily higher gun pressure (80.9 ρ%) and secondarily longer spray distance (13.5 ρ%) would result in a smoother coating finish. The Taguchi evaluation at 300 A indicated that using the lower level for the gun traverse rate would

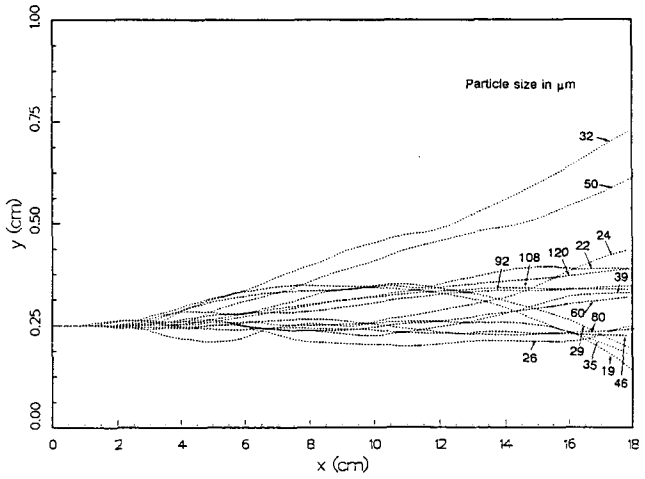

Fig. 3 Predicted particle cluster trajectories for Experiment TA04

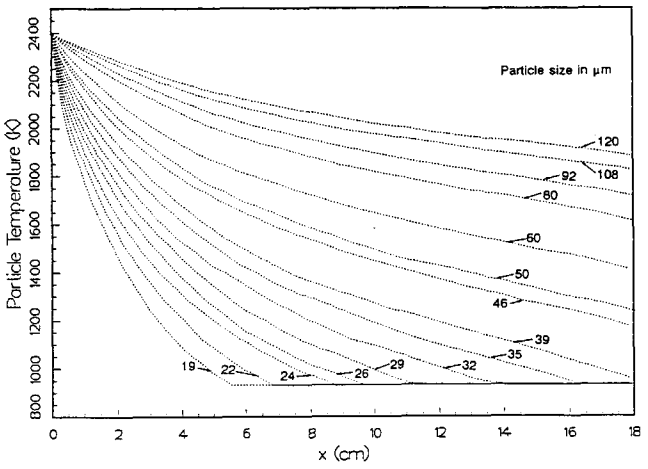

Fig. 4 Predicted particle cluster temperatures as a function of axial location in the plume for Experiment TA04

have the most significant impact, lowering roughness at 70.9 ρ%. Spray distance had a 20.6 ρ%, with the longer standoff (177.8 mm, or 7 in.) resulting in smoother coatings.

Superficial hardness (i.e., Rockwell) was increased equally by the use of a lower level of gun pressure (38.6 ρ%) and the upper level of gun traverse rate (36.8 ρ%) at 150 A. The Taguchi evaluation at 250 A indicated that longer spray distance (60.7 ρ%) would result in a harder coating. Using the lower level for the gun pressure (75.7 ρ%) and the upper level for traverse rate (23.4 ρ%) would increase hardness at 300 A.

An increase in microhardness (i.e., Vickers) was influenced most by a lower level of gun pressure at 150 A. Using the upper level for gun traverse rate dominated the hardness increase at 250 A. The Taguchi evaluation at 300 A indicated that the lower levels for gun pressure (49.4 ρ%) and spray distance (42.4 ρ%) would result in harder coatings.

The Taguchi evaluation indicated that spray distance completely dominated other process parameters for deposition efficiency. Shorter spray distance resulted in higher deposition efficiency; 96.6, 93.9, and 99.5 ρ% were obtained for the 150, 250, and 300 A experiments, respectively.

Selection of the optimum levels of design factors can produce an optimum coating for this particular application. This coating would have low porosity, high thickness, low roughness, high hardness, and high deposition efficiency. This coating can be obtained by using a gun pressure of 345 kPa (50 psia), air flow of 50.5 l/min, spray distance of 177.8 mm (7 in.), and traverse rate of 381 mm/s (15 in./s) for all three power levels.

5. Numerical Modeling of the Twin-Wire Electric Arc Process

A spray-laden gas flow can be numerically modeled using spray models embedded in computational fluid dynamic (CFD) codes. Such codes typically compute the Eulerian gas flow field along with a set of Lagrangian-based particle flight patterns. Such particle flight paths may represent either a single particle or a cluster of particles. Fluid dynamic and particle models derived to represent the dynamics of a dilute dispersed phase in a gas flow field have been proposed by Crowe, Sharma, and Stock,[8] Gosman and Ioannides,[9] and Zhou and Yao,[10] among others.

The main features of the model of Zhou and Yao[10] have been implemented in a two-dimensional, compressible, axisymmetric, turbulent flow CFD code. The code belongs to the TEACH (Gosman and Ideriah)[11] family of codes and uses the standard *k-e* turbulence model. Conditions approximating the spray from a twin-wire electric arc spray gun have been modeled using the spray code. The inlet conditions for the spray codes are obtained by idealizing the liquid spray-laden gas flow as it leaves the gun. Flow from the exit jet is assumed to be fully expanded with centerline Mach numbers equalizing 0.95 and seeded with a distribution of liquid droplets from 19 to 120 mm at 2400 K.

The model of Zhou and Yao assumes that clusters of same size particles travel in flight paths that are characteristic of a single particle of that size. The local spatial distribution of particles in the cluster is assumed to be Gaussian and to disperse radially from the cluster center as it travels downstream. Their model also allows the turbulence to affect the flight path of the cluster by superimposing a random turbulent velocity on the mean particle velocity.

Experiment TA04 was modeled. Figure 3 illustrates the flight paths of 15 clusters of pure aluminum particles within the aforementioned size range. As the particles travel toward the target, they lose thermal energy to the surrounding air. The code models the energy loss based on the local Reynolds numbers of the particles. The material in each cluster of particles is assumed to be at a uniform temperature. Figure 4 illustrates the drop in temperature of each particle cluster as a function of axial distance. The temperature of each particle decreases until it reaches the solidification temperature and then remains constant as the material solidifies. The smaller particles lose energy faster because they have less mass to cool. The mass fraction of particles that have reached the solidification temperature before hitting the target is about 40%. Although this CFD spray code uses the main features of the model of Zhou and Yao, the model should be de-

veloped further to yield results that agree satisfactorily with experimental data.

The BUILD[12] coating dynamics computer program used in this study uses the particle data generated by the CFD code at the standoff distance to calculate the dynamics of the coating buildup. The code calculates the morphology of the injected particles one at a time and accumulates the results. As the particles are accumulated into the coating calculational matrix, the code calculates the coating thickness, porosity, and the average temperature and velocity of the impacting particles in the coating matrix.

The thickness of sample TA04, measured with image analysis, was 396 μm (15.6 mils) and the porosity was 4.7%. The BUILD code calculated a thickness of 373 μm (14.7 mils) and a porosity of 3.7%. For the 552 particles that hit the matrix, the average temperature and velocity were 1256 K and 54 m/s, respectively. Of the 552 particles, 369 were between 19 and 24 μm in diameter, 78 were between 24 and 29 μm, 54 were between 29 and 50 μm, and 51 were between 50 and 120 μm.

6. Summary and Conclusion

An experimental study of the twin-wire electric arc spraying of aluminum wire has been presented. Experiments used a Taguchi fractional factorial approach with typical process parameters. The coatings were characterized by hardness tests, surface roughness, and optical metallography. Coating qualities were determined with respect to thickness, roughness, hardness, porosity, deposition efficiency, and microstructure.

The aluminum coating thicknesses ranged from 81 to 255 μm/pass (3.2 to 10 mils/pass). Porosity for the coatings, as revealed by image analysis, ranged from 2.7 to 6.2%. The superficial Rockwell hardness measurements ranged from 23 to 60, whereas the microhardness measurements ranged from 41.7 to 52.6. The deposition efficiencies ranged from 46.3 to 57.8%. The roughness of the coatings ranged from 5.52 to 7.65 μm.

The Taguchi evaluation indicated that, to lower porosity, the higher level for spray distance should be used at 150 A, higher levels for gun pressure and spray distance should be used at 250 A, and the higher gun pressure should be used at 300 A. The Taguchi evaluation at 150 and 250 A indicated that the lower level for the gun traverse rate was the most significant contributor to increasing thickness. At 300 A, the lower level for the spray distance was the most significant contributor to increasing thickness. Surface roughness was influenced most by the higher level gun pressure at 150 and 250 A. At 300 A, the lower level for traverse rate would have the most significant impact on lowering roughness. Increased superficial hardness (i.e., Rockwell) was equally influenced by the lower level for gun pressure and the higher level for the gun traverse rate at 150 A. At 250 A, the higher level spray distance would result in harder coatings. Using the lower level for gun pressure (75.7 ρ%) and the higher level for the gun traverse rate (23.4 ρ%) would increase hardness at 300 A. Increased microhardness was influenced most by using the lower level for gun pressure at 150 A, the higher level for the traverse rate at 250 A, and the lower level for gun pressure and spray distance at 300 A. The lower level for spray distance resulted in higher deposition efficiency for all three Taguchi experiments. An optimum coating for this particular application can be obtained by using a gun pressure of 345 kPa (50 psia), a spray distance of 177.8 mm (7 in.), and a traverse rate of 381 m/s (15 in./s) for all three powers.

The numerical model of the process, which included gas, droplet, and coating dynamics, is considered to be a first approximation of the dynamics occurring in the process. Further development of the model will be required before it will yield results that correlate more satisfactorily with experimental data.

The objective of this and future work is to optimize aluminum coatings. The range of coating attributes generated through the methodology presented in this article serves to optimize the process and ultimately the coatings. From this statistical methodology, processing parameters can be adjusted, optimized, and confirmed, and reliable and repeatable coating specifications can be established. The procedure described herein will also assist in selecting and optimizing operational parameters for future metal thermal spray processing experiments and applications for the twin-wire electric arc process.

Acknowledgments

The technical input provided by V.L. Smith-Wackerle, INEL, is gratefully acknowledged. The work described in this article was supported by the US Department of Energy under DOE Idaho Operations Office Contract No. DE-AC07-76ID01570.

References

1. E.D. Kubel, Thermal Spray Technology: From Art to Science, *Adv. Mater. Proc.*, Vol 132(No. 6), 1987, p 69-80
2. E. Pfender, Fundamental Studies Associated with the Plasma Spray Process, *Thermal Spray: Advances in Coatings Technology*, D.L. Houck, Ed., ASM International, 1992, p 1-10
3. P. Fauchais, J.F. Coudert, A.M. Vardelle, A. Grimaud, and P. Roumilhac, State of the Art for the Understanding of the Physical Phenomena Involved in Plasma Spraying at Atmospheric Pressure, *Thermal Spray: Advances in Coatings Technology*, D.L. Houck, Ed., ASM International, 1992, p 11-21
4. T.J. Steeper, D.J. Varacalle, Jr., G.C. Wilson, A.J. Rotolico, J.E. Nerz, and W.L. Riggs, A Taguchi Experimental Design Study of Plasma Sprayed Alumina-Titania Coatings, *J. Thermal Spray Technol.*, Vol 2 (No. 3), 1993, p 251-256
5. T.J. Steeper, D.J. Varacalle, Jr., G.C. Wilson, and V.T. Berta, Use of Thermal Spray Processes to Fabricate Heater Tubes for Use in Thermal-Hydraulic Experiments, *Thermal Spray Coatings: Properties, Processes, and Applications*, T.F. Bernecki, Ed., ASM International, 1992, p 425-432
6. G. Taguchi and S. Konishi, *Taguchi Methods: Orthogonal Arrays and Linear Graphs*, ASI Press, 1987
7. R.F. Culp, *SADIE*, 1989
8. C.T. Crowe, M.P. Sharma, and D.E. Stock, The Particle-Source-In-Cell (PSI-Cell) Model for Gas-Droplet Flows, *J. Fluids Eng.*, Vol 99(No. 6), 1977, p 325-332
9. A.D. Gosman and E. Ioannides, *Aspects of Computer Simulation of Liquid-Fueled Combustors*, AIAA, AIAA-81-0323, Jan 1981
10. Q. Zhou and S.C. Yao, *A Group Model for Particle Dispersion in Turbulent Sprays, Heat and Mass Transfer in Fires and Combustion Systems*, HTD-148, ASME, 1990, p 27-32
11. A.D. Gosman and F.J.K. Ideriah, "TEACH—2E: A General Computer Program for Two-Dimensional, Turbulent, Recirculating Flows," Department of Mechanical Engineering, Imperial College, London, 1976
12. D.J. Varacalle, Jr. and W.L. Riggs, Analytically Modeling the Plasma Spray Deposition of Tribaloy 800, *Thermal Spray Coatings: Properties, Processes, and Applications*, T.F. Bernecki, Ed., ASM International, 1992, p 245-250